

Published in final edited form as:

Biomed Signal Process Control. 2009 October 1; 4(4): 302–308. doi:10.1016/j.bspc.2009.01.008.

Adaptive Bolus-chasing Computed Tomography Angiography in the Cases of Symmetric and Asymmetric Arterial Flows in Peripheral Arteries

Zhijun Cai¹, Ge Wang², and Er-Wei Bai¹

¹ Department of Electrical and Computer Engineering, University of Iowa, Iowa City, IA, 52242

² VT-WFU School of Biomedical Engineering & Sciences, Virginia Polytechnic Institute & State University, Blacksburg, VA 24061, USA

Abstract

Synchronization of the contrast bolus peak and CT imaging aperture is a crucial issue for computed tomography angiography (CTA). It affects the CTA image quality and the amount of contrast dose. A whole-body CTA procedure means to scan from the abdominal aorta to pedal arteries. In this context, the synchronization is much more difficult with the asymmetric arterial flow in lower extremities than in the case of symmetric arterial flow. In this paper, we propose an adaptive optimal controller to chase the contrast bolus peak while it propagates in the aorta and lower extremities with symmetric flow. In the case of asymmetric flow after the contrast bolus splitting into two lower limbs, we propose a dynamic programming approach to cover the lower limbs optimally. Simulation and experimental results show that the proposed methods outperform the current constant-speed method substantially.

Keywords

Adaptive optimal control; medical imaging systems; computed tomography angiography (CTA); dynamic programming; peripheral arteries; asymmetric flow

1. Introduction

Vascular disease includes any condition that affects the human circulatory system, such as cardiovascular disease and peripheral artery disease. The former is related to the No. 1 cause of the death of Americans, heart disease, and the latter is affecting more than five million Americans' lives [1,2,3]. Recently, Computed Tomography Angiography (CTA) has become an important investigative tool for vascular disease with the advent of multi-row CT [4,5]. To better define the vasculature from its surrounding soft tissue, a dose of contrast medium (a contrast bolus) is injected into a vein through an IV (intravenous) tube. During the scanning, the contrast bolus propagates in the artery, and meanwhile the patient is fed into the CT gantry by translating the CT table. It is highly desirable to scan the blood vessels with the highest density contrast bolus inside. Therefore, synchronizing the contrast bolus peak and CT imaging aperture is crucial to the CTA scan results. Unfortunately, the contrast bolus dynamics are

Publisher's Disclaimer: This is a PDF file of an unedited manuscript that has been accepted for publication. As a service to our customers we are providing this early version of the manuscript. The manuscript will undergo copyediting, typesetting, and review of the resulting proof before it is published in its final citable form. Please note that during the production process errors may be discovered which could affect the content, and all legal disclaimers that apply to the journal pertain.

highly nonlinear, complicated, and influenced by many factors, e.g., patient weight, vascular diseases, and injection patterns. In current clinical practice, the CT table moves at a preset constant speed, and is very likely to miss the bolus peak. To compensate for this problem, a large amount of contrast medium is needed; however, it is harmful to the patient's kidney [6].

The currently existing bolus chasing techniques only mean to chase the bolus arrival, which determines CT table starting time. Those techniques can be categorized into two main classes: Region Of Interest (ROI) threshold triggering [7,8] and the timing bolus [9,10]. The former technique sets a threshold (in the unit of Hounsfield Unit or HU, which represents the bolus density) at a specific position, e.g., aorta, which is being monitored after the injection. When the observed bolus density reaches the threshold, the CT table is automatically started. Unfortunately, it is very difficult for the operators to choose the correct threshold [11]. If it is set too low, the CT table will be started too early. If it is set too high, the CT table might not be started at all. The other technique calls for an injection of a small amount contrast medium prior to the main injection used for diagnosis. The time between the injection to the vein and peak density appearance in the ROI is taken as the delay time (may be added by several seconds) to start the CT table for the main injection. Obviously, it is assumed that the timing bolus and actual bolus have the same peak arrival time, which may not be true in most cases [7]. Furthermore, it requires an additional injection and test time, which increases the contrast dose and the diagnosis time.

Even when the accurate bolus arrival time to the designated ROI is obtained, there is no guarantee of the synchronization of the bolus peak and imaging aperture during the CT exam due to the complicated bolus dynamics. Consequently, many researchers try to make the resulting bolus profile more conducive to the preset constant-speed method by means of varying the injection rate and duration, called bolus geometry optimization method [8,12,13,14,15]. It is expected that if a bolus keeps its maximum density for a longer time at a position, then the synchronization is easier to be obtained. As a result, many injection protocols were reported, such as multiple-injection method [16] and the inverse method [14]. However, these methods require a priori knowledge of the patient vascular system to achieve the desirable results and it is impossible to know that knowledge before a preliminary injection. To that end, it may end up with a larger amount of contrast dose, which is not good for patients.

The importance of the synchronization of contrast bolus and imaging aperture has been realized in [17,18]. In [18], Laswed and his colleagues used different table speed for different patient based on the bolus aorta-popliteal transit time of each individual, and they reported that in such a way, the vasculature CT image qualities are improved. However, this is not the ultimate solution for bolus chasing, 1) the test bolus dynamics are different from that of the main bolus and 2) constant speed during the scanning will not synchronize the bolus peak and x-ray aperture optimally due to the nonlinear dynamics of the bolus.

The effective and robust way to chase the bolus peak is the adaptive method, which predicts the bolus peak using the real time CT images and varies the CT table speed accordingly. This concept has been studied in other imaging modalities, such as Digital Subtraction Angiography (DSA) [19] and Magnetic Resonance Angiography (MRA) [20,21]. Preferable results have been reported in these studies. However, there are few studies on bolus chasing CTA due to the small field of view (z direction) for CTA and the complicated CT image reconstruction algorithm with varying pitch. Recently, we have developed the CT image reconstruction algorithms for varying pitch [22] and extensively studied the bolus characteristics [23,24].

To scan the whole body of a patient is more difficult due to the small diameter vessels in the lower limbs and the asymmetric flow. Figure 1 shows the human arterial tree. It is easy to see that there is one main artery, aorta, in part A, while there are two main artery branches in part

B. For a patient with Peripheral Artery Diseases (PAD), it is likely that the arterial flow in the lower limbs is asymmetric; hence, sticking to chase the contrast bolus in one lower limb means missing to scan the other lower limb. Rubin and his colleagues are the pioneers to study the CTA on peripheral arteries. In his study [25], seven of twenty-four patients have at least one location where the difference in right-left (leg) arterial attenuation was greater than 38 HU, and the maximum difference can reach 96 HU. Of all these seven patients, asymmetric arterial diseases are present. The authors state “when severe asymmetries exist, the diagnostic quality of the initial angiographic examination can be limited and thus necessitate repeated selective injections of contrast medium”. Therefore, an effective CTA scan method is called for in clinical.

The paper is organized as follows: in Section 2, adaptive bolus chasing algorithm is presented. In Section 3, we discuss dynamic approach for asymmetric flow in lower limbs. Section 4 gives the experimental results for whole-body CTA scan, followed by discussion and conclusion in Section 5.

2. Adaptive optimal controller for bolus chasing computed tomography angiography

An effective CTA scan method includes two parts: 1) optimally chasing the bolus peak in one main artery, and 2) effectively switching to chase the bolus peaks in two artery branches when asymmetric arterial flow happens. In this section, we focus on the first problem.

Problem Statement

The overall goal of the adaptive bolus chasing CTA is to design an adaptive controller to synchronize the bolus peak and imaging (x-ray) aperture. It is achieved by instantaneously processing the bolus CT images, dynamically predicting the bolus peak position, and adaptively moving the CT table in the opposite direction of the blood flow. Let the bolus density function be given by $B(t, z)$, where t represents time ($t=0$ corresponds to the injection instant) and z represents distance ($z=0$ corresponds to the initial monitored position). Also let the scan range

be divided into N segments, that is, $z_k = k \frac{L}{N}$, $k = 1, \dots, N$, where L is the scan distance. The control objective is to find a time sequence, $\{t^*(z_k)\}_{k=1}^N$, such that

$$J_c = \sum_{i=1}^N B(t^*(z_i), z_i) \quad (1)$$

is maximized, under the constraint of maximum and minimum velocity of the CT table, or equivalently

$$0 < \Delta_s \leq t(z_{k+1}) - t(z_k) \leq \Delta_b < \infty \quad (2)$$

where Δ_s and Δ_b are determined by CT table maximum and minimum speed, respectively. The motivation behind (1) is to maximize the average enhancement over the whole scan length, which results in overall better quality CTA images for every position of the blood vessel.

Controller design

Before we design the adaptive optimal controller, the contrast bolus characteristics are carefully studied [23]. Here, we give its most important property concerning the controller design: At any given position z , the bolus density $B(t, z)$ is monotonically (not necessarily strictly) increasing in time t before it reaches the maximum and is monotonically (not necessarily strictly) decreasing after that. Since this property is frequently used in the paper, we define such a function as a class \mathcal{A} function.

Definition 1—A differentiable function $f(t)$ is said to belong to the class \mathcal{A} if t^*

1. There exists a maximum point t^* such that $t^* = \arg \max_t f(t)$.
2. $f(t)$ is monotonically (not necessarily strictly) increasing for $t = (-\infty, t^*]$ and monotonically (not necessarily strictly) decreasing for $t = [t^*, \infty)$.

In case that $B(t, z)$ is known, Let

$$t^*(z_k) = \arg \max_t B(t(z_k), z_k) \quad k=1, \dots, N \quad (3)$$

The control law is given by

$$t_k^* = \begin{cases} t_k^* = t_{k-1}^* + \Delta_s, & \text{if } t^*(z_k) \leq t_{k-1}^* + \Delta_s \\ t_k^* = t_{k-1}^* + \Delta_b, & \text{if } t^*(z_k) \geq t_{k-1}^* + \Delta_b \\ t_k^* = t^*(z_k), & \text{otherwise} \end{cases} \quad (4)$$

where $t^*(z_k)$ is given in (3).

However, $B(t, z)$ is unknown during the tracking, and we have to estimate it and modify the control law as follows.

Let $\hat{B}_{k-1}(t, z)$ be the estimated bolus model at step $k-1$ and

$$\bar{t}(z_k) = \arg \max_t \hat{B}_{k-1}(t, z_k) \quad k=1, \dots, N \quad (5)$$

The control law is modified as follows

$$\bar{t}_k = \begin{cases} \bar{t}_k = \bar{t}_{k-1} + \Delta_s, & \text{if } \bar{t}(z_k) \leq \bar{t}_{k-1} + \Delta_s \\ \bar{t}_k = \bar{t}_{k-1} + \Delta_b, & \text{if } \bar{t}(z_k) \geq \bar{t}_{k-1} + \Delta_b \\ \bar{t}_k = \bar{t}(z_k), & \text{otherwise} \end{cases} \quad (6)$$

where $\bar{t}(z_k)$ is given in (5).

The final tracking error between $B(t_k^*, z_k)$ and $B(\bar{t}_k, z_k)$ bounded by the estimation error between $B(t, z_k)$ and $\hat{B}_{k-1}(t, z_k)$, and the difference of t_k^* and \bar{t}_k , See [26] for details.

Online estimation of $B(t, z)$

Since $B(t, z)$ is unavailable, calculation of the control law relies on the estimates $\hat{B}_{k-1}(t, z_k)$. As shown in the previous subsection, if the estimate $\hat{B}_{k-1}(t, z_k)$ is close to the true but unknown $B(t, z)$ locally, the effect of approximation is negligible. However, $\hat{B}_{k-1}(t, z_k)$ has to be estimated in real time solely based on the observed local bolus information. On one hand, the approximation error depends on how rich the structure of the approximation $\hat{B}_{k-1}(t, z_k)$ is that incorporates well the local bolus information into its representation. On the other hand, the structure should be simple enough so that it can be easily estimated on line. There is a trade off between approximation ability and estimation accuracy. A natural choice of $\hat{B}_{k-1}(t, z_k)$ is a polynomial. The order of the polynomial balances the ability to approximate $B(t, z)$ and the estimation simplicity. We consider a second order polynomial,

$$B(t, z) \approx B(t_k, z_k) + \nabla_t B|_{(t_k, z_k)}(t - t_k) + \nabla_z B|_{(t_k, z_k)}(z - z_k) + \frac{1}{2} \begin{pmatrix} t - t_k \\ z - z_k \end{pmatrix}^2 \nabla^2 B|_{(t_k, z_k)} \begin{pmatrix} t - t_k \\ z - z_k \end{pmatrix} \\ = a_0 + a_1 t + a_2 z + a_3 t^2 + a_4 t z + a_5 z^2 \quad (7)$$

for some a_0, a_1, a_2, a_3, a_4 and a_5 , which will be estimated on line. Another important factor is the selection of approximation data. Obviously, the smaller the region, the better a second order polynomial can approximate $B(t, z)$. On the other hand, we would like the approximation function to give us some information about the bolus away from the observation points. This implies that the approximation region cannot be too small. In addition, realistic CT specifications have to be considered.

- CT is assumed to have multiple rows of detectors.
- CT gantry rotation speed is set to $\Delta T = 1/3$ second per rotation, a standard in modern CT.
- The maximum patient table speed in a modern CT is about 10 cm/sec [4], which sets the lower bound Δ_s in the constraint.
- The minimum speed is set to 0 cm/sec which ensures that the patient table does not go back, a standard practice. This sets the upper bound Δ_b .

With these constraints, data points of $B(t, z)$ at $\bar{t}_k, \bar{t}_{k-1}, \bar{t}_{k-2}$ and $z = z_k, z = z_k \pm \delta z$ are collected for each rotation of the gantry. These data are used to identify the a_i 's in the second order approximation in the least squares sense

$$\hat{a}_i = \arg \min_{a_i} \sum_{z=z_k, z_k \pm \delta z, t=\bar{t}_k, \bar{t}_{k-1}, \bar{t}_{k-2}}^3 \left\{ B(t, z) - (a_0 + a_1 t + a_2 z + a_3 t^2 + a_4 t z + a_5 z^2) \right\}^2 \quad (8)$$

Further, the next \bar{t}_{k+1} is determined from (6) with

$$\hat{B}_k(t, z_{k+1}) = \hat{a}_0 + \hat{a}_1 t + \hat{a}_2 z_{k+1} + \hat{a}_3 t^2 + \hat{a}_4 t z_{k+1} + \hat{a}_5 z_{k+1}^2. \quad (9)$$

Simulation results

The proposed adaptive optimal chasing algorithm has been tested on the actual clinical data collected from UIHC and NU. In all the simulations, the upper and lower bounds $\Delta_b, \Delta_s, \Delta T$,

and L/N are set as 10 cm/s, 0 cm/s, 1/3 seconds and 5 mm, respectively. Both the proposed method against the existing technology, constant-speed method, i.e., $t_k = cz_k + t_0$, (c is constant), are evaluated in terms of performance index (PI), defined as

$$I_a = \frac{\sum B(t^*, z_k)}{\sum B(t^*(z_k), z_k)}, I_a = \frac{\sum B(cz_k, z_k)}{\sum B(t^*(z_k), z_k)} \quad (10)$$

where c is set to 1/3 sec/cm, i.e., the CT table speed is at 3 cm/sec [1]. $\Sigma B(t^*(z_k), z_k)$ is the maximum achievable bolus density. $\Sigma B(t^*, z_k)$ and $\Sigma B(cz_k, z_k)$ are the actually achieved bolus densities for the adaptive method and the constant-speed method respectively.

Figure 2 shows the typical tracking results for both adaptive and constant-speed method, where the top plot shows the bolus contour (solid thin curve: the inner the curve, the higher the density), the bolus peak trajectory (dashed), adaptive bolus chasing trajectory (solid) and constant-speed trajectory (dash dot); and the bottom plot shows the maximum achievable bolus density at each position z_k (dashed), the achieved bolus density by the adaptive method (solid) and the achieved bolus density by the constant-speed method (dash dot). Table 1 summarizes the PI for ten patients. Clearly, in all cases the proposed adaptive method outperforms the current constant-speed method significantly.

3. Dynamic programming approach for asymmetric arterial flow in lower limbs

Although the adaptive bolus chasing method ensures the highest possible contrast to noise ratio (CNR) for every cross-sectional slice of a single artery, such as aorta, the method itself cannot guarantee a good coverage when the contrast bolus splits into the lower limbs and asymmetric arterial flow happens, which is very often for PAD patient. When the asymmetric flow happens, it is very unlikely that the arteries in both lower limbs of the same position (z -direction, especially in the distal position) are enhanced simultaneously; therefore, tracking the contrast bolus in one lower limb consistently means a great chance to lose coverage for the other lower limb. To that end, scanning strategy has to be modified while tracking the contrast bolus in the lower extremities. In this section, we propose a dynamic programming approach for bolus chasing CTA on asymmetric arterial flow in lower limbs.

Dynamic programming approach

The problem of scanning the lower extremities is due to the unbalanced contrast bolus movement in both lower limbs, which basically makes it hard to obtain a good scan results for both lower limbs. Theoretically, by moving CT table back and forth quickly enough, we can scan both lower limbs with satisfactory enhancement. But unfortunately, there is a speed constraint on the CT table, and when and how to move the CT table back/forth needs to be determined carefully. The dynamic programming (DP) is then proposed to approach this problem. Before illustrating the dynamic programming approach idea, we need to make some assumptions.

- The contrast bolus peak velocities in both lower limbs are known, which makes it easier to present the results. As for the scenario with unknown bolus velocities, it is much harder and will be our future work.
- Our purpose at this moment is to scan each part of the lower limb with high enhancement.

- The maximum speed (v_{Tm}) of the CT table is known. The patients' discomfort, related to the acceleration, is not considered at this stage.
- Physicians have a priori knowledge of the scanning priority of each part of the lower limbs. For example, a PAD patient may have a higher chance to have stenosis in the left thigh and therefore the resulted scanning strategy must ensure the left thigh to be fully scanned. The scanning priority is realized by assigning weights to each part of the lower limbs. The higher the weight of the part, the higher the scanning priori that part is.

The dynamic programming approach is described as follows. First, we divide each lower limb into N partitions as shown in Figure 3, and each part is represented by its center point/node, denoted by L_i or R_i , $i = 1, 2 \dots, N$. We assume that if a node is scanned, then the whole part centered at that node will be scanned with a reasonable CNR. Further, each node is assigned a weight according to its scanning priority (not order), $W(L_i)$ or $W(R_i)$, $i = 1, 2 \dots, N$. Then the problem of scanning two lower limbs is converted into an optimization problem with cost function as

$$J = \sum W(P_k), \text{ where } P_{k+1} = f(p_k, k) \quad (11)$$

Under the constraint of causality and maximum speed of the CT table. In (11), f is the table control strategy, which is the solution of the optimization problem and determines which node $P_k \in \{L_1, \dots, L_N, R_1, \dots, R_N\}$ should be covered and when. This is a two branch dynamic programming problem, which can be solved efficiently.

Since the contrast bolus velocities in both lower limbs are known, the bolus arrival time at each node can be derived and denoted by $t(L_i)$ or $t(R_i)$. Now, we can put all the nodes on both lower limbs in the ascending order of bolus arrival time, that is, $t(P_i) > t(P_j) \Rightarrow i < j$. The cost function value at node j is given by

$$J_j = \max_{i < j} \{J_i + W(P_i), W(P_i)\}, \frac{|P_i - P_j|}{|t(P_i) - t(P_j)|} \leq v_{Tm} \quad (12)$$

It is a standard dynamic programming problem and numerical solutions are available in [28].

The algorithm is summarized as follows

1. Divide each lower limb into N parts and assign weight to each part.
2. Find the maximum cost function value at each node using algorithm (12).
3. The solution is obtained by tracking the highest cost function value node down to the starting node.

Remark 1

1. How to divide each lower limb and how many parts are optimal is the problem related to the clinical practice. We will not discuss it here.
2. The solution may not be unique.

3. Moving CT table back and forth results in additional radiation exposure compared to the conventional scan. However, if asymmetric arterial flow happens, conventional scan needs another scan for the uncovered leg. The proposed method actually helps to minimize the radiation exposure to cover both legs in a possible way.

This dynamic programming approach is able to cover several scenarios for chasing the contrast bolus into two lower limbs. If one is interested in the artery of the left lower limb, $W(L_i) = N$ and $W(R_i) = 1$ may be assigned and in such a way, the resulted scan strategy guarantees the left lower limb be scanned fully only if the bolus speed is less than the maximum CT table speed. If one is interested in one or several part a lower limb, the weights for those nodes could be increased.

Simulation results

To demonstrate dynamic programming approach on the two-leg CTA scan problem, three different scenarios are simulated. In all the following simulations, each lower limb is 100 centimeters, which is the average length of a normal male adult. Each lower limb is divided into $N = 10$ parts and each part is represented by its center. The lower bolus velocity is set to 2 cm/sec, and the maximum CT table speed is 15 cm/sec. Without loss of generality, we assume the bolus flows faster in the left lower limb and the slower bolus runs in the right lower limb. Dynamic programming approach is applied for three cases of two-leg CTA scan problem: 1) scanning priorities are the same for all nodes on both lower limbs. In this case, we also compared the scanning scheme for different bolus speed ratio. 2) Higher scanning priority for one lower limb (either the left lower limb or the right lower limb). 3) Higher scanning priority for part of one lower limb.

Case 1: The same weights on all nodes of the both lower limbs—In this case, we assume there is no scanning priority on both lower limbs, therefore; all the nodes of both lower limbs are assigned the same weight, one. As expected, the dynamic programming approach results depend on the speed ratio of faster and slower bolus. When the speed ratio is low (the top plot of Figure 4), CT table is moving back and forth to cover both lower limbs as much as possible; However, when the speed is high (the bottom plot of Figure 4), the left lower limb (the faster bolus) is scanned first and then switch to the right lower limb (the slower bolus). Simulation results for speed ratio between 1.2 and 2 are listed in Table 2. It is interesting that the total weight is not monotonically decreasing as the speed ratio increase. The reason is that the close bolus arrival times of two nodes on different lower limbs prevent them being scanned one after the other.

Case 2: Higher weight on one lower limb—In some cases, physicians might have priori information of the PAD and know which lower limb is likely to have diseases. Then this is easy to approach by assign a higher weight on that lower limb. For example, if the left lower limb is preferred to be covered fully, we can assign N to each node on the left lower limb and keep weight 1 on the node on the right lower limb. The top and bottom plot of Figure 5 show the dynamic programming results for higher weight on the right lower limb and the left lower limb, respectively. In both cases, the speed ratio is 1.2. It is clear that all the nodes on the left lower limb are scanned in the top plot and all the nodes on the right lower limb are scanned in the bottom plot. Although the total weights for both cases are the same, 108, the locations (y axis) of missing nodes are different.

Case 3: Higher weight on part of the lower limb—The weights of the nodes on one lower limb can be different, which corresponds to the cases when physicians are interested in some specific parts of the lower limbs and want to scan the rest of the lower limb as much as possible. To simulate that, we first set the weights of the middle two nodes on the left lower limb to 2, and use the dynamic programming approach. The result is shown in the top plot of

Figure 6, and then we set the weights of the middle two nodes on the right lower limb to 2, the corresponding result is shown in the bottom plot of Figure 6. In both cases, the higher weighted nodes are scanned, and the rest of the nodes are covered as many as possible under the dynamic programming approach.

4. Experimental results

The proposed adaptive bolus chasing CTA method including resulted scan strategy is implemented on the vasculature phantom using our in-house Siemens SOMATOM Volume Zoom CT scanner with four-detector rows. Figure 7 shows the vasculature phantom used in the bolus chasing experiment. The contrast bolus is mixed with red dye and driven by a programmable pump, which controls the flow rate inside the vasculature phantom. Haemostatic forceps are used to vary the bolus speed ratio in two lower limbs for asymmetric flow. During the scan, the bolus cross-sectional image is shown on the monitor by real time image reconstruction algorithms. A frame grabber is used to capture the CT images and feed the bolus information to the controller. The controller predicts the bolus peak position at the next sampling time, and sends a command to move the table accordingly. Thus, the bolus peak is kept right under the CT imaging aperture.

Due to the proprietary issues, we are unable to fulfill our control scheme fully. First, real time raw data is not available, and secondly, CT table control is through the CANbus line, which causes control delay [27]. To that end, we have to scale down the flow rate of the contrast and we can not demonstrate the complicated tracking strategy. In this experiment, we will demonstrate the tracking strategy to cover the left lower limb (faster bolus) and then cover the right lower limb as much as possible. The results are shown in Figure 8, where the top plot shows the scanned Hounsfield Unit of left and right lower limb and the bottom plot shows the CT table movement trajectory. We can see that both lower limbs are covered well except some misses between 460 ~ 520 mm of the right lower limb, while the constant speed method (set as 2cm/sec, which is optimal for the faster bolus) misses the whole right lower limb (Figure 9).

It is noticed that the uncovered segment lies in the upper part of the right leg. This can be explained as follows: when the contrast bolus splits into two legs, their peaks are not separated immediately, but after a while, they are far away from each other due to the asymmetrical arterial flow. The CT scans the faster leg till the end and then and then come back to scan the right leg, in which the contrast bolus flows slower. However, as the CT table is moved back for the right leg, the bolus contrast in the right leg already flows some distance ahead, though slowly, and that distance cannot be covered any more in this scan.

Remark 2

1. Hounsfield Unit is transformed back from the pixel value on the screen. Because we do not have real time raw data, a frame grabber is used, which transform the HU into pixel values between 0–255. In order to have better resolution of the bolus, we set the CT display center at 400 and window 150. To that end, any position with HU close to 150 in Figure 8 top plot and Figure 9 means it is not enhanced well.
2. The HU curve in Figure 8 top plot is smoother than that in Figure 9. This is because adaptive chasing method moves at a big step every time due to the control delay, while the constant speed method moves the CT table continuously.

5. Discussion and conclusion

The asymmetric arterial flow in the lower extremities is mostly caused by peripheral arterial stenosis in only one leg or different positions in two legs. Arterial occlusion is the extreme case of the stenosis. It blocks the arterial flow to the downstream. The proposed approach is also applicable to the occlusion case though it is not demonstrated in the experiment. We can either treat it as one main artery case (neglect the occluded leg) or set the velocity of arterial flow in the occluded leg be very low and still use the DP approach. Both methods need some prior information of the vasculature. The later one is more conservative but increases the radiation exposure.

We simulate the asymmetric flow on a vasculature phantom. The flow pattern may not be the same as that in the human body. Actually, it is unknown before/after the experiment. However, it is good enough to demonstrate the control scheme, which claims to be able to track the bolus peak without knowing the actual bolus dynamics.

In summary, we propose an adaptive optimal method to track the contrast bolus peak in one main artery and dynamic programming approach for the asymmetric arterial flow in peripheral arteries, which form a whole body CTA scan scheme. Simulation results show that the proposed method outperforms the existing constant-speed method substantially. Experiments on the Siemens CT scanner successfully demonstrate the proposed whole-body scan scheme, which will be the promising CT techniques for vascular diseases.

References

1. Selvin E, Erlinger TP. Prevalence of and risk factors for peripheral arterial disease in the United States: Results from the National Health and Nutrition Examination survey, 1999–2000. *Circulation* 2004;110:738–43. [PubMed: 15262830]
2. Hirsch AT, Haskal ZJ, et al. ACC/AHA Guidelines for the Management of Patients with Peripheral Arterial Disease (lower extremity, renal, mesenteric, and abdominal aortic): a collaborative report from the American Associations for Vascular Surgery/Society for Vascular Surgery, Society for Cardiovascular Angiography and Interventions, Society for Vascular Medicine and Biology, Society of Interventional Radiology, and the ACC/AHA Task Force on Practice Guidelines (writing committee to develop guidelines for the management of patients with peripheral arterial disease)--summary of recommendations". *J Vasc Interv Radiol* 2006;17(9):1383–97. quiz 1398. [PubMed: 16990459]
3. Becker GJ, McClenny TE, et al. The importance of increasing public and physician awareness of peripheral arterial disease. *J Vasc Interv Radiol* 2002;13(1):7–11. [PubMed: 11788688]
4. Fuchs TOJ, Kachelriebe M, Kalender WA. Fast Volume Scanning Approaches by X-Ray-Computed Tomography. *Proceedings of the IEEE* 2003;91(10):1492–1502.
5. Jakobs T, Wintersperger B, Becker C. MDCT Imaging of Peripheral Arterial Disease. *Seminars in Ultrasound, CT, and MRI* 2004;(25)(2):145–155.
6. Bae KT. Technical aspects of contrast delivery in advanced CT. *Supplement to Applied Radiology* 2003;32:12–19.
7. Cademartiri F, van der Lugt A, et al. Parameters affecting bolus geometry in CTA: a review. *J Comput Assist Tomogr* 2002;26(4):598–607. [PubMed: 12218827]
8. Schweiger GD, Chang PJ, Brown BP. Optimizing contrast enhancement during helical CT of the liver: a comparison of two bolus tracking techniques. *AJR Am J Roentgenol* 1998;171(6):1551–1558. [PubMed: 9843287]
9. Hittmair K, Fleischmann D. Accuracy of Predicting and Controlling Time-Dependent Aortic Enhancement from a Test Bolus Injection. *Journal of Computer Assisted Tomography* 2001;25(2):287–294. [PubMed: 11242230]
10. Bae KT. Test-bolus versus bolus-tracking techniques for CT angiographic timing. *Radiology* 2005;236(1):369–70. author reply 370. [PubMed: 15987987]

11. Paulson EK, Fisher AJ, DeLong DM, Parker DD, Nelson RC. Helical liver CT with computer assisted bolus-tracking technology: Is it possible to predict which patients will not achieve a threshold of enhancement. *Radiology* 1998;209:787–792. [PubMed: 9844675]
12. Bae KT, Heiken JP, Brink JA. Aortic and hepatic peak enhancement at CT: effect of contrast medium injection rate--pharmacokinetic analysis and experimental porcine model. *Radiology* 1998;206(2):455–64. [PubMed: 9457200]
13. Backer CR, Hong C, Knez A, Leber A, Bruening R, Schoepf UJ, Reiser MF. Optimal contrast application for cardiac 4-detector-row CT. *Investigative Radiology* 2003;38(11):690–694. [PubMed: 14566178]
14. Fleischmann D, Hittmair K. Mathematical analysis of arterial enhancement and optimization of bolus geometry for ct angiography using the discrete Fourier transform. *Journal of Computer Assisted Tomography* 1999;23(3):474–484. [PubMed: 10348458]
15. Kopka L, Rodenwaldt J, Fischer U, Mueller DW, Oestmann JW, Grabbe E. Dual-phase helical CT of the liver: Effects of bolus tracking and different volumes of contrast material. *Radiology* 2004;201:321–326. [PubMed: 8888218]
16. Rossi P, Baert A, et al. Multiple bolus technique vs. single bolus or infusion of contrast medium to obtain prolonged contrast enhancement of the pancreas. *Radiology* 1982;144(4):929–931. [PubMed: 7111749]
17. Laswed T, Rizzo E, et al. Assessment of occlusive arterial disease of abdominal aorta and lower extremities arteries: value of multi-detector CT angiography using an adaptive acquisition method. *European Radiology* 2008;18(2):263–72. [PubMed: 17899108]
18. Fleischmann D, Rubin GD. Quantification of intravenously administered contrast medium transit through the peripheral arteries: implications for CT angiography. *Radiology* 2005;236(3):1076–82. [PubMed: 16000649]
19. Wu, Z.; Qian, J. Real-time tracking of contrast bolus propagation in X-ray peripheral angiography. *IEEE Workshop on Biomedical Image Analysis*; Santa Barbara, CA. 1988.
20. Wang Y, Lee HM, et al. Bolus-chase MR digital subtraction angiography in the lower extremity. *Radiology* 1998;207(1):263–269. [PubMed: 9530326]
21. Ho VB, Choyke PL, et al. Automated bolus chase peripheral MR angiography: initial practical experiences and future directions of this work-in-progress. *J Magn Reson Imaging* 1999;10(3):376–388. [PubMed: 10508299]
22. Yu H, Ye Y, Zhao S, Wang G. A backprojection filtration algorithm for nonstandard spiral cone-beam CT with an n-PI-window. *Physics in Medicine and Biology* 2005;50(9):2099–2111. [PubMed: 15843739]
23. Cai Z, Stolpen A, et al. Bolus characteristics based on Magnetic Resonance Angiography. *Biomed Eng Online* 2006;5:53. [PubMed: 17044929]
24. Bennett J, Bai E, et al. A Preliminary Study on Adaptive Field-of-View Tracking in Peripheral Digital Subtraction Angiograph. *J of X-ray Science and Technology* 2003;11:149–159.
25. Rubin GD, Schmidt AJ, Logan LJ, et al. Multi-detector row computed angiography of lower extremity arterial inflow and runoff: initial experience. *Vasc and Interv Radiol* 2001;221:146–158.
26. Bai EW, Cai Z, et al. An Adaptive Optimal Control Design for a Bolus Chasing Computed Tomography Angiography. *IEEE Transactions on Control Systems Technology* 2008;16(1):60–69.
27. Cai Z, Erdahl C, et al. Adaptive bolus chasing computed tomography angiography: Control scheme and experimental results. *Biomedical Signal Processing and Control* 2008;3(4):319–326. [PubMed: 19802329]
28. Bellman, Richard. *Dynamic Programming*. Princeton University Press; 1957.

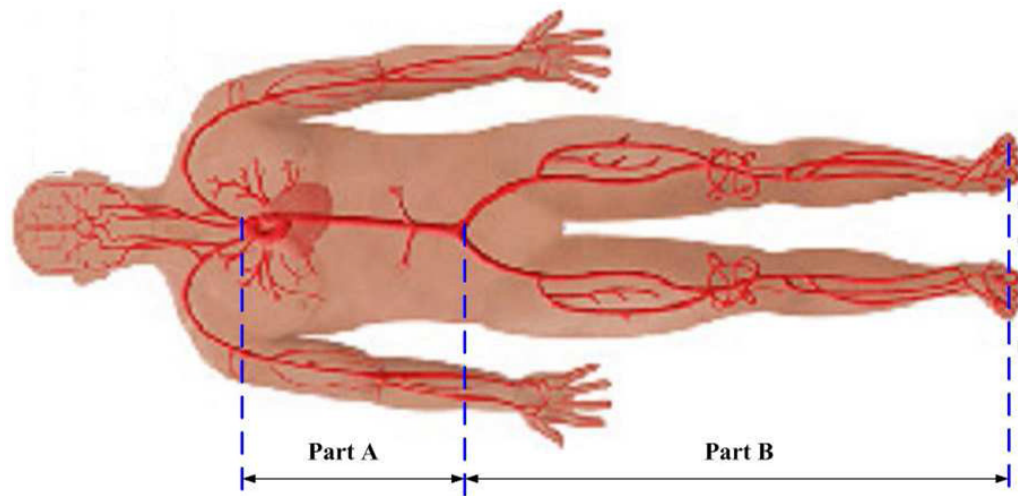


Figure 1.
The human arterial tree. Part A includes the aorta, and Part B includes common iliac artery, femoral artery, popliteal artery, posterior tibial artery and anterior tibial artery.

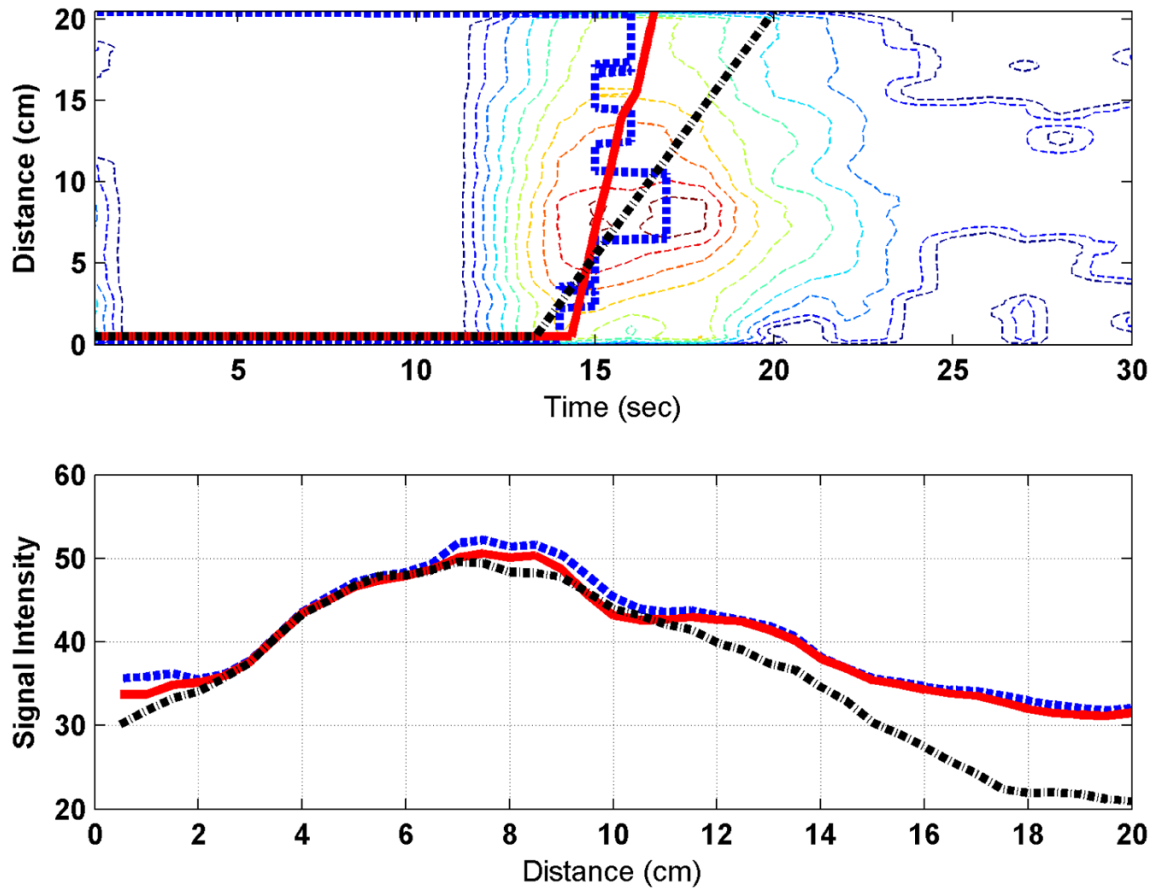


Figure 2.

Tracking result on a patient data collected from UIHC. Top plot: the adaptive (solid) and constant-speed (dash dot) method trajectory on the bolus contour (solid thin curve). The bolus peak trajectory is denoted by dashed curve. Bottom plot: the achieved bolus density by the adaptive (solid) and constant-speed (dash dot) method, the maximum achievable bolus the achieved density is denoted by dashed curve.

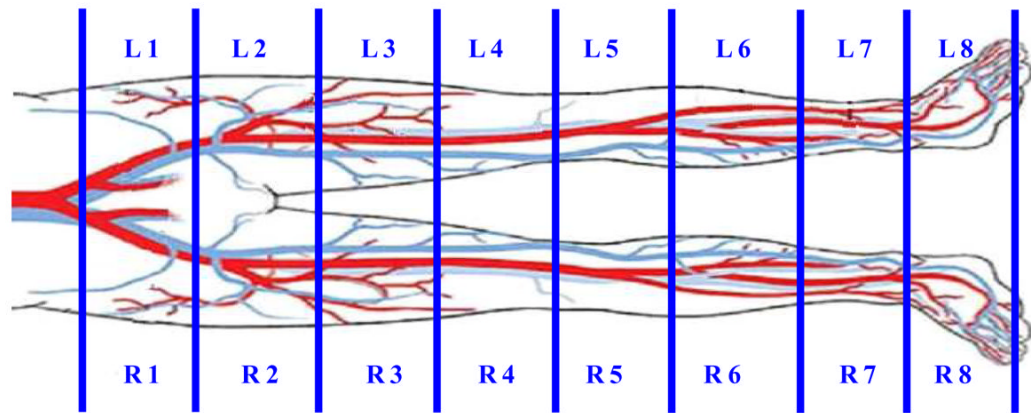


Figure 3.
Each lower limb is divided into eight parts.

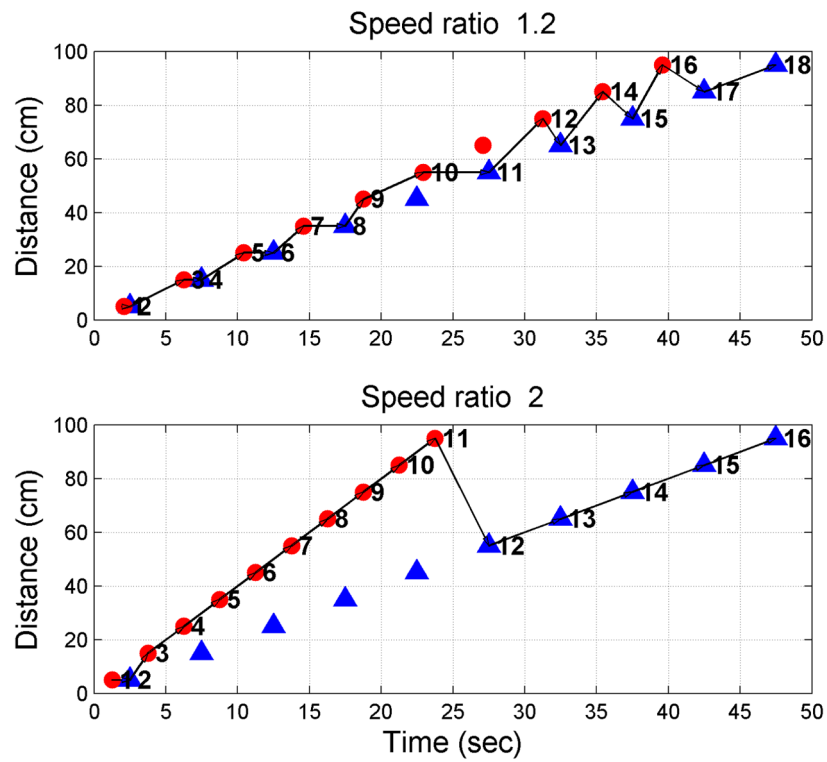


Figure 4. Scanning arrangement results of dynamic programming approach on two-leg scan problem for speed ratio 1.2 (top plot) and speed ratio 2 (bottom plot). In both plots, dots denote nodes on the left lower limb and triangles denote the nodes on the right lower limb. Numbers beside each dot denote the accumulated weight from the beginning to that node.

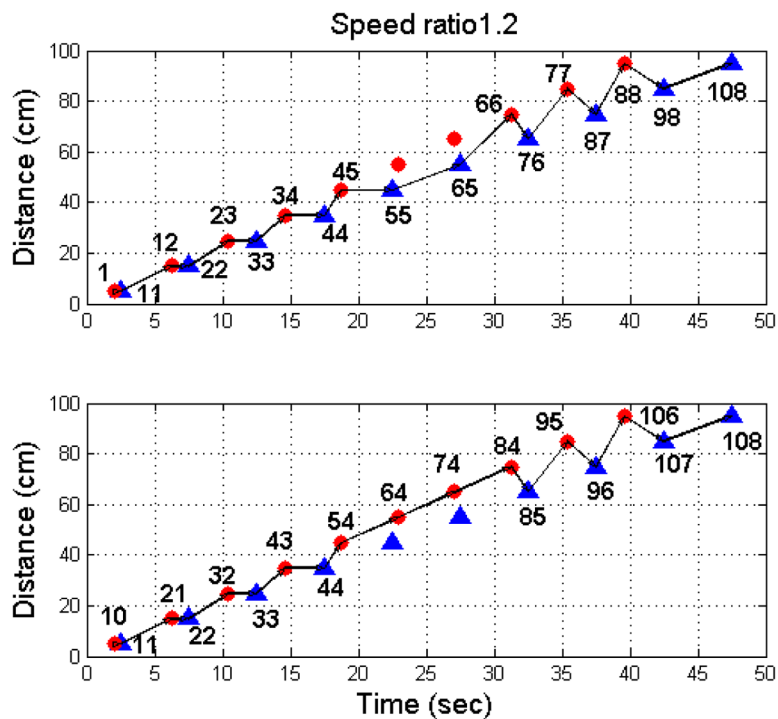


Figure 5. Scanning arrangement results of dynamic programming approach on two-leg scan problem for higher weight on right lower limb (the top plot) and higher weight on the left lower limb (bottom plot). In both plots, speed ratio is 1.2, and dots denote nodes on the left lower limb and triangles denote the nodes on the right lower limb. Numbers beside each dot denote the accumulated weight from the beginning to that node.

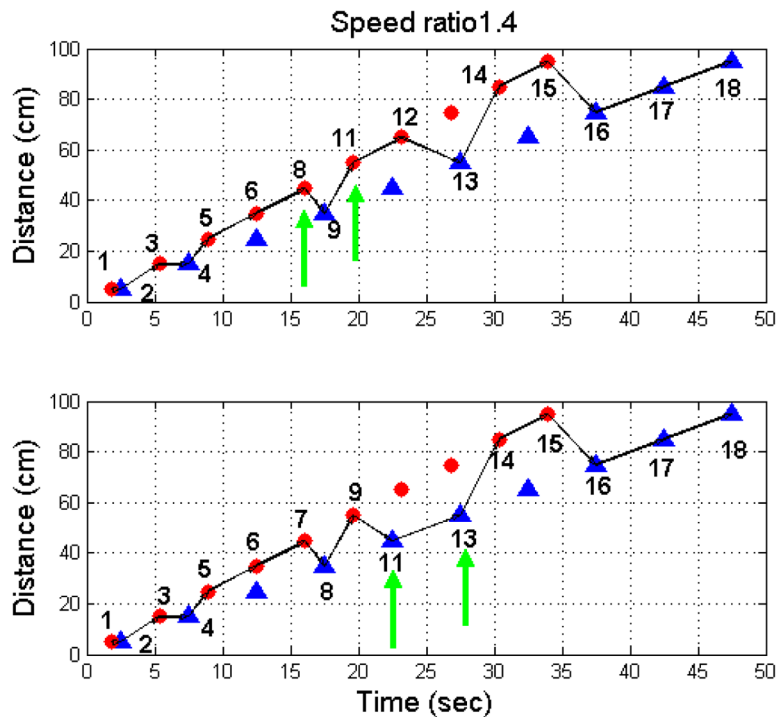


Figure 6. Scanning arrangement results of dynamic programming approach on two-leg scan problem for higher weights of the middle two nodes on left lower limb (top plot) and the right lower limb (bottom plot). In both plots, speed ratio is 1.4, and dots denote nodes on the left lower limb and triangles denote the nodes on the right lower limb. Numbers beside each dot denote the accumulated weight from the beginning to that node. The green arrows point to the node with weight 2.



Figure 7.
The vasculature phantom in the bolus chasing experiment.

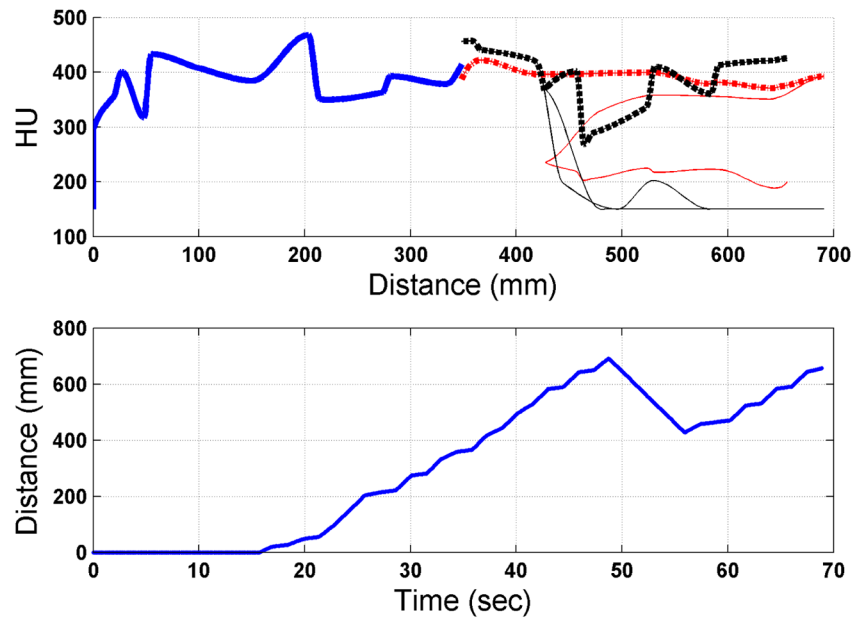


Figure 8. Adaptive bolus chasing CTA experimental results. Top plot: scanned Hounsfield Units for the aorta (blue thick solid), the left lower limb (red thick dashed) and the right lower limb (black thick dash dot), both lower limbs are scanned under a relatively high HU. Bottom plot: the CT table movement trajectory. It tracks the faster bolus first and then comes back to track the slower bolus.

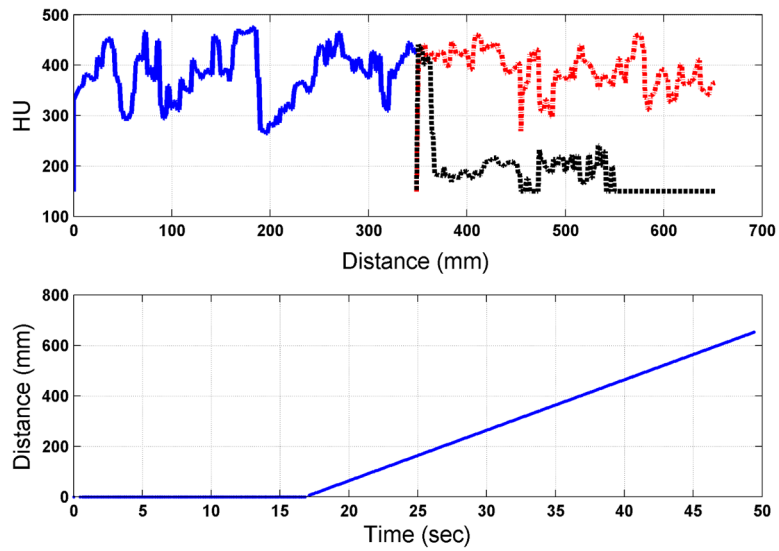


Figure 9.

Constant-speed method results of CTA scan. CT table moves at 2 cm/sec, which is derived from the Figure 8. Top plot: scanned Hounsfield Units for the aorta (blue thick solid), the left lower limb (red thick dotted) and the right lower limb (black thick dash dot). Bottom plot: the CT table movement trajectory. The constant-speed method covers the left lower limb well but misses the right lower limb totally.

Table 1

Performance index of adaptive method and constant-speed method on clinical data sets collected from UIHC and NU.

UIHC patient	I_a	I_c	NU patient	I_a	I_c
Patient 1	0.98	0.90	Patient 1	0.99	0.93
Patient 2	0.95	0.78	Patient 2	0.98	0.85
Patient 3	0.93	0.74	Patient 3	0.97	0.81
Patient 4	0.95	0.83	Patient 4	0.99	0.90
Patient 5	0.93	0.84	Patient 5	0.98	0.58

Table 2

Dynamic programming approach results for different speed ratio of faster and slower bolus.

Speed ratio	Number of node NOT scanned	Total weight
1.2	2	18
1.3	3	17
1.4	4	16
1.5	4	16
1.6	4	16
1.7	5	15
1.8	5	15
1.9	4	16
2.0	4	16